Predicting lightning-driven quasi-electrostatic fields at sprite altitudes using in situ measurements and a numerical model

Jeremy N. Thomas, Robert H. Holzworth, and Michael P. McCarthy
Department of Earth and Space Sciences, University of Washington, Seattle, Washington, USA

Osmar Pinto Jr.
National Institute of Space Research (INPE), São Jose dos Campos, São Paulo, Brazil

Received 9 February 2005; revised 17 March 2005; accepted 25 April 2005; published 24 May 2005.

[1] Data from the largest electric field change (>140 V/m) above 30 km ever published, correlated with two positive cloud-to-ground (+CG) strokes, are compared with an axi-symmetric quasi-electrostatic field (QSF) model developed by the authors and based on the model of Pasko et al. (1997a). Using the best fit parameters of this comparison, the electric field change everywhere in the stratosphere and mesosphere is predicted and compared to various electrical breakdown thresholds needed for the initiation and/or growth of sprites. **Citation:** Thomas, J. N., R. H. Holzworth, M. P. McCarthy, and O. Pinto Jr. (2005), Predicting lightning-driven quasi-electrostatic fields at sprite altitudes using in situ measurements and a numerical model, *Geophys. Res. Lett.*, *32*, L10809, doi:10.1029/2005GL022693.

1. Introduction

[2] Since the first image of sprites was recorded in 1989 [*Franz et al.*, 1990], there have been numerous experimental and theoretical studies which have attempted to determine the underlying physics of the phenomena. The first experimental studies focused on optical imaging [*Sentman et al.*, 1995; *Lyons*, 1994] and the classification of the visual characteristics of sprites. Latter studies involving the meteorology of sprite producing storms determined that sprites were correlated with positive cloud-to-ground (+CG) lightning and most often occurred during large scale storms known as mesoscale convective systems (MCS) or complexes (MCC) [*Lyons*, 1996]. The more recent studies have explored the electric and magnetic fields associated with sprites and their parent lightning discharges [*Cummer et al.*, 1998; *Bering et al.*, 2002; *Sato et al.*, 2003]. This had been accomplished primarily by ground based RF measurements (ULF to VLF) of the waveforms of the sprite-parent strokes, and occasionally the sprites themselves [*Cummer et al.*, 1998; *Sato et al.*, 2003]. The first in situ campaign that attempted to measure the electric and magnetic fields in the stratosphere above sprite producing thunderstorms failed to make measurements in the near field region of sprites or lightning [*Bering et al.*, 2002], although, electric and magnetic field changes correlated with sprites and sprite-parent lightning were measured at distances greater than 300 km.

[3] Models have been developed to try to explain the mechanism for sprite production [*Roussel-Dupre and Gurevich*, 1996; *Pasko et al.*, 1997a; *Lehtinen et al.*, 1997; *Rowland*, 1998]. A well accepted model involves a quasi-static field that forms after a large positive cloud-to-ground stroke [*Pasko et al.*, 1997a], which if large enough, can cause electrical breakdown in the atmosphere. However, before this study, these models had only been directly compared to electric fields measured below about 16 km in altitude above +CG producing storms [*Marshall et al.*, 1996]. In this paper, a +CG driven electric field change is simulated using a numerical QSF model and compared with the measured in situ field change in the stratosphere. Then, input parameters that best fit the data are used to predict the quasi-electrostatic field at sprite altitudes.

2. Data Set

[4] The data used in this study are in situ balloon measurements of electric fields (dc to VLF) and atmospheric conductivity from the Brazil Sprite Campaign 2002–2003 [*Thomas et al.*, 2004; *Holzworth et al.*, 2005], along with the ground based Brazilian Integrated Lightning Network (BIN) [*Holzworth et al.*, 2005, Figure 1] and remote ELF magnetic field measurements courtesy of M. Sato and Tohoku University [*Sato et al.*, 2003]. These in situ electric fields were determined using the double Langmuir probe technique, which measured the voltage difference between pairs of conductors isolated via high input impedance operational amplifiers [*Thomas et al.*, 2004]. Two balloon payloads each equipped with these electric field sensors flew over or near intense thunderstorm activity in the southeast of Brazil on Dec. 6–7, 2002 and March 6–7, 2003. In addition to determining the electric field, one pair of Langmuir probes measured the conductivity of the atmosphere every 10 min. [*Holzworth et al.*, 2005, Figure 4] using the relaxation technique [*Holzworth and Bering*, 1998]. Unfortunately, the view of the aircraft based imaging cameras was blocked by clouds, so sprites could not be observed during the balloon flights. However, sprites were imaged at other times during the campaign when there were no balloon flights [*Pinto et al.*, 2004].

3. Model Formulation

[5] The numerical QSF model developed for this study uses an axi-symmetric cylindrical coordinate system

0094-8276/05/2005GL022693$05.00

centered about the lightning stroke and is based on the model of *Pasko et al.* [1997a]. The model uses a one km resolution 2-d grid, with altitude Z = 0–90 km and radial distance R = 0–60 km, to simulate the lightning-driven electric field pulse in the 3-d space encompassed by this 90 km × 120 km cylinder. This model assumes that the CG stroke removes charge from the cloud without any orientation (vertical or horizontal) of the lightning current identified, with the coordinate system origin (R = 0, Z = 0) at the location of the detected ground stroke. Moreover, only the electric field change due to lightning events is realistically modeled, not the background electric field before and after the lightning events, which involves complicated cloud charging/discharging mechanisms [*Rakov and Uman*, 2003, chap. 3].

[6] The cloud is charged with a characteristic charging time t_c (0.5 s for the case study in section 4) to a charge density of $\rho_c = \rho_+ + \rho_-$ where ρ_+ and ρ_- are each Gaussian distributions (in both the Z and R coordinates) of positive and negative charge layers normalized to $\pm Q_0$ (total positive or negative charge). Charge is removed from the positive layer (+CG) or negative layer (−CG) with time t_d to simulate the lightning stroke. At each time step the background charge density ρ_b (which is initialized as $\rho_b = 0$) and the cloud charge density ρ_c are used to solve for the electric field $\vec{E}$ using the Poisson equation

$$\nabla \cdot \vec{E} = \frac{(\rho_b + \rho_c)}{\epsilon_0} \quad (1)$$

with Z = 0, 90 km and R = 60 km assumed to be perfect conductors. The background charge density is evolved in time due the non-zero, altitude dependent atmospheric conductivity σ (the sum of ion and electron contributions to conductivity) and electric field E (solved in (1)) by a modified continuity equation [*Pasko et al.*, 1997a]

$$\frac{\partial \rho_b}{\partial t} + \nabla\sigma \cdot \vec{E} + \frac{\rho_b \sigma}{\epsilon_0} = 0 \quad (2)$$

where ϵ_0 the permittivity of free space.

[7] The atmospheric conductivity below 60 km in altitude is dominated by ions [*Volland*, 1984, chap. 2] and increases exponentially ($\sigma_i = \sigma_{i0} e^{z/h}$) with altitude z and scale heights of h = 8 and 11.1 km (below and above 40 km respectively) as measured by balloon- and rocket-borne instruments in the middle atmosphere [*Holzworth et al.*, 1985]. This ion conductivity profile is confined to fit the in situ data measured during Sprite Flight 1 to solve for σ_{i0}. Above 60 km the electron conductivity dominates, and is determined by $\sigma_e = eN_e\mu_e$ where e is the electron charge, N_e is the electron density, and μ_e is the electron mobility. The electron density profile increases exponentially with a scale height of 3 km with N_e(60 km) = 5 × 10^3 m^{-3} which is similar to the electron density profile model employed by *Pasko and Inan* [1994, Figure 4, profile 1]. The electron mobility is dependent on the neutral atmospheric density N (given by the MSIS-E-90 model (http://nssdc.gsfc.nasa.gov/space/model/models/msis.html) for the exact location and time of measurements) and the electric field due to the lightning discharge E, and it is solved for self-consistently using an empirical fit [*Pasko et al.*, 1997a] to experimental data [*Davies*, 1983; *Hegerberg and Reid*, 1980] through the form

$$\mu_e = 1.36 N_0/N, \text{ for } EN_0/N < 1.62 \times 10^3 \text{V/m} \quad (3)$$

$$\mu_e = 10^{\sum_{i=0}^{2} a_i x^i}/N, \text{ for } EN_0/N \geq 1.62 \times 10^3 \text{V/m}$$

where x = log(E/N), a_0 = 50.970, a_1 = 3.0260, a_2 = 8.4733 × 10^{-2}, and N_0 = 2.4901 × 10^{25} m^{-3} is the neutral density at sea level. Hence, (3) shows that when the effective electric field (EN_0/N) is greater than 1.62 × 10^3 V/m, the electrons are heated by the electric field thus lowering the electron mobility. When the effective electric field is below this heating threshold, the electron conductivity employed in this study agrees relatively well with rocket measurements of mesospheric electron conductivity [*Hale et al.*, 1981].

4. Case Study

[8] This case study compares the QSF model to a +CG event that was measured by the Sprite Flight 1 electric field sensor at an altitude of 34 km. This +CG event is comprised of two +CG strokes that occurred at ∼00:00:09 UT Dec. 7, 2002 ∼140 ms apart at a horizontal distance of ∼34 km from the balloon payload. These +CG strokes had estimated peak currents of +15 kA and +53 kA, as determined by BIN, with a total combined charge moment of 329–1683 C-km estimated (using both the fitting and impulse methods) from remote ELF measurements in Antarctica and Japan [*Sato et al.*, 2003].

[9] Figure 1 one shows the comparison between the model output at R = 34 km and Z = 34 km and in situ data for this +CG event, composed of two +CG strokes at 0.50 s and 0.64 s, for both the vertical (Figure 1 (top)) and radial (Figure 1 (bottom)) electric fields. Note that the time interval 0.0–0.5 s is the artificial cloud charging time t_c for the QSF model. In this coordinate system, a negative vertical electric field represents a field vector pointing towards the ground. The dc (<25 Hz) electric field data are shown in Figure 1. The dc and ac (not shown) electric field data for this event had similar rise times which confirms that the dc instrument properly measured the initial rise of the field.

[10] The model parameters that best fit model to data for this event (comprised of two +CG strokes) within ±10% are: total charge moment of 479 ± 50 C-km (152 C-km for the first +CG stroke and 327 C-km for the second +CG stroke), discharge times of 100 ms for the first +CG stroke and 8 ms for the second +CG stroke, charge layer diameter of 59 ± 17 km (same for positive and negative layer), charge layer thickness of 1.4 ± 0.5 km (for the positive and negative layers separately), positive charge layer altitude of 6 km, negative charge layer altitude of 4 km, and atmospheric conductivity as defined in section 3 with ion conductivity constants of σ_{i0} = 9 × 10^{-14} (Ωm)$^{-1}$ and 3.4 × 10^{-13}(Ωm)$^{-1}$ (below and above 40 km respectively) to match with the ion conductivity measured by Sprite Flight 1 (6 × 10^{-12} (Ωm)$^{-1}$ average total conductivity for the 12 hr flight [see *Holzworth et al.*, 2005, Figure 4]). The model and data agree well for the rise and initial decay of

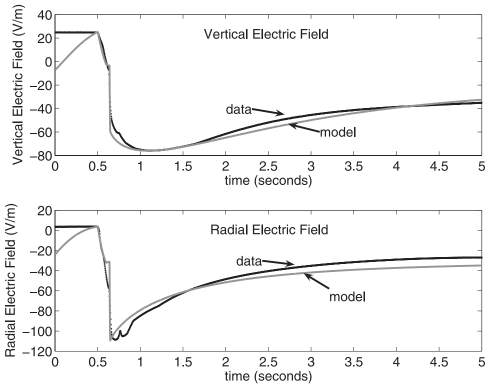

Figure 1. Comparison between model (grey line) at R = 34 km and Z = 34 km and data (black points) for two +CG strokes at 0.50 s and 0.64 s. (top) Vertical electric field. (bottom) Radial electric field.

the electric field change (0.5–1.5 s), thus showing that a QSF approach is effective in modeling lightning driven electric fields. However, since the complex cloud charging/discharging processes not related to the +CG event are not included in this model, the electric field before the first +CG stroke (which occurs at 0.5 s) and well after the two discharges (1.5 s) are less well correlated.

[11] These best fit parameters are now used to predict the lightning-driven electric field perturbation at higher altitudes where sprite initiation and/or growth can occur. Figure 2 shows the QSF model output for the vertical electric field driven by two +CG strokes at 500 ms and 640 ms at R = 0 km, Z = 50, 60, 70, 80 km using these parameters. In Figure 3, the vertical electric field magnitude vs. altitude is shown at three instants in time (1 ms before the first +CG stroke, 1 ms after the second +CG stroke, and 350 ms after the second +CG stroke) and compared to the various electric breakdown thresholds. The electric field is maximum just after the second +CG stroke (pointing downward) but never surpasses the conventional breakdown threshold E_k. The vertical electric field does surpass the positive streamer breakdown threshold E_{cr}^+ for Z = 66–82 km and the relativistic breakdown threshold E_t for Z =

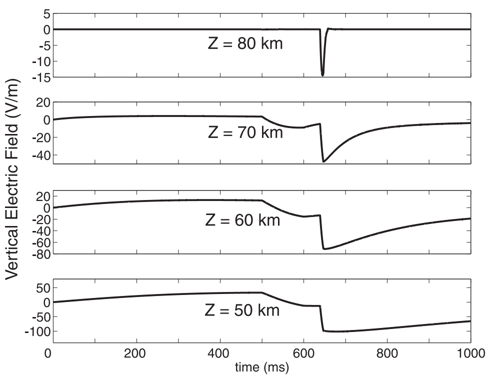

Figure 2. Model prediction of the vertical electric field driven by two +CG strokes at 500 ms and 640 ms at four different mesospheric altitudes (Z = 80, 70, 60, and 50 km, R = 0 km) using best fit parameters to the measured electric field change at Z = 34 km, R = 34 km.

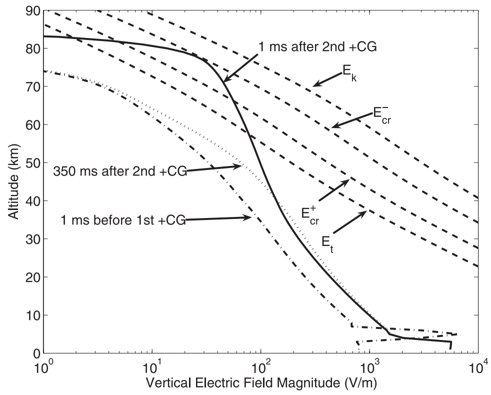

Figure 3. Model prediction of the vertical electric field magnitude vs. altitude at R = 0 km using best fit parameters to the measured electric field change at Z = 34 km, R = 34 km. The vertical electric field magnitude at three instants in time (1 ms before the first +CG stroke, 1 ms after the second +CG stroke, and 350 ms after the second +CG stroke) is compared to the various breakdown thresholds (E_k [*Raizer*, 1991], E_{cr}^- [*Babaeva and Naidis*, 1997], E_{cr}^+ [*Allen and Ghaffar*, 1995], E_t [*Marshall et al.*, 1995]).

58–83 km, and the field approaches the negative streamer breakdown threshold E_{cr}^- at Z = 77 km (to within 94%). Note that due to the 1 km grid spacing employed in the model, the electric field in the cloud (altitude <8 km) is not well resolved. At 1 ms before the first +CG stroke, the field should be zero at two altitudes in the cloud, at 3–4 km and again at 6–7 km in Figure 3. Since this QSF model does not attempt to accurately model in-cloud fields, this lack of resolution has no effect on this analysis.

5. Discussion and Conclusions

[12] For the first time, lightning-driven electric field changes measured in situ above 30 km have been compared directly to a numerical QSF model. The agreement between model and data for the rise and initial decay of the vertical and radial electric field perturbations suggests that the QSF approach is valid for modelling lightning driven fields. The large diameter (59 km) and thin (1.4 km), low altitude (6 km for the positive layer and 4 km for the negative layer) charge layers agree with previous studies involving large charge moment +CG events which are usually associated with MCC/MCS storms [*Marshall et al.*, 1996; *Williams*, 1998]. The storm that generated the +CG in this case study had an area of 5000–10000 km^2 (estimated from GOES satellite IR images), which is at the lower limit for MCS storm size. The positive and negative charge layers employed in the QSF model had an area of about 2700 km^2, about 25–50% of the total storm area.

[13] Although sprites were not confirmed for the +CG event in this case study, the implications of the predicted electric fields in the mesosphere can be examined. The relaxation time of the mesospheric electric field change is predicted to be at least as long as the duration of a typical sprite event (τ = 69 ms at Z = 70 km) allowing for sufficient time for sprite initiation and/or growth. Yet, since the electric field after the +CG event never surpasses the conventional breakdown threshold E_k, sprite initiation

would not occur for this model prediction. Although the relativistic threshold E_t is surpassed above 58 km in altitude, optical emissions would not be initiated by an upward relativistic electron beam since only a few avalanche lengths (*e*-foldings of the electron population) would be able to develop with this high of a starting altitude [*Roussel-Dupre and Gurevich*, 1996, Figure 10]. However, if the electric field was to surpass the conventional threshold E_k at a typical sprite initiation altitude of about Z = 78 km [*Wescott et al.*, 2001] due to processes not included in this model, i.e. gravity waves [*Pasko et al.*, 1997b] or micrometeors [*Wescott et al.*, 2001], then sprites could readily propagate downwards from the initiation altitude since the positive streamer threshold E_{cr}^{+} is surpassed for Z = 66–82 km. Also, since the negative streamer threshold E_{cr}^{-} is nearly surpassed near Z = 78 km, propagation upward from the initiation altitude could occur in the region.

[14] The downward direction of the electric field is determined by the positive polarity of the CG event which allows the positive streamer to propagate downward to about Z = 66 km. If instead this was a negative polarity CG event, the field would point upward and the positive streamer would propagate upward to about Z = 82 km. Thus, the positive polarity of the CG event would allow for sprites, once initiated, to have a much larger vertical extent ($\sim Z$ = 66–78 km) compared to a sprite caused by a −CG ($\sim Z$ = 78–82 km). This difference in breakdown thresholds for positive and negative streamer production could partially explain why sprites are almost exclusively correlated with positive polarity lightning. Although, for sufficiently large charge moments, both the positive and negative streamer thresholds would be surpassed, and thus the direction of propagation and vertical extent of the sprites would not depend on the polarity of the parent lightning stroke.

[15] Clearly, future in situ electric field measurements of confirmed sprite events, used together with a numerical QSF model, could provide much insight into the physical mechanisms underlying the initiation and growth of sprites.

[16] **Acknowledgments.** This work was supported by the US National Science Foundation under grants ATM-0091825 and ATM-0355190 to the University of Washington and by the Brazilian government FAPESP project 02/01329-1 to the Brazilian National Institute for Space Research (INPE). The authors thank M. Sato (RIKEN, Japan) and Tohoku University for estimating charge moments from their ELF measurements. J.N.T. thanks V. Pasko (Penn. St. U.) for helping with the development of the QSF model.

References

Allen, N. L., and A. Ghaffar (1995), The conditions required for the propagation of a cathode-directed positive streamer in air, *J. Phys. D Appl. Phys.*, *28*, 331–337.

Babaeva, N. Y., and G. V. Naidis (1997), Dynamics of positive and negative streamers in air in weak uniform electric fields, *IEEE Trans. Plasma Sci.*, *25*, 375–379.

Bering, E. A., III, J. R. Benbrook, J. A. Garrett, A. M. Paredes, E. M. Wescott, D. R. Moudry, D. D. Sentman, H. C. Stenbaek-Nielsen, and W. A. Lyons (2002), The electrodynamics of sprites, *Geophys. Res. Lett.*, *29*(5), 1064, doi:10.1029/2001GL013267.

Cummer, S. A., U. S. Inan, T. F. Bell, and C. P. Barrington-Leigh (1998), ELF radiation produced by the electrical currents in sprites, *Geophys Res. Lett.*, *25*, 1281–1284.

Davies, D. K. (1983), Measurements of swarm particles in dry air, in *Theoretical Notes*, *Note 346*, Westinghouse R&D Cent., Pittsburgh, Pa.

Franz, R. C., R. J. Nemzek, and J. R. Winckler (1990), Television image of a large electrical discharge above a thunderstorm system, *Science*, *249*, 48–51.

Hale, L. C., C. L. Croskey, and J. D. Mitchell (1981), Measurements of middle atmospheric electric fields and associated electrical conductivities, *Geophys Res. Lett.*, *8*, 927–930.

Hegerberg, R., and I. D. Reid (1980), Electron drift velocities in air, *Aust. J. Phys.*, *33*, 227–230.

Holzworth, R. H., and E. A. Bering (1998), Ionospheric electric fields from stratospheric balloon-borne probes, in *Measurement Techniques in Space Plasmas: Fields*, *Geophys. Monogr. Ser.*, vol. 103, edited by R. F. Pfaff, J. E. Borovsky, and D. T. Young, pp. 79–84, AGU, Washington, D. C.

Holzworth, R. H., M. C. Kelley, C. L. Siefring, L. C. Hale, and J. D. Mitchell (1985), Electrical measurements in the atmosphere and the ionosphere over an active thunderstorm: 2. Direct current electric fields and conductivity, *J. Geophys Res.*, *90*, 9824–9830.

Holzworth, R. H., M. P. McCarthy, J. N. Thomas, J. Chin, T. M. Chinowsky, M. J. Taylor, and O. Pinto Jr. (2005), Strong electric fields from positive lightning strokes in the stratosphere, *Geophys. Res. Lett.*, *32*, L04809, doi:10.1029/2004GL021554.

Lehtinen, N. G., T. F. Bell, V. P. Pasko, and U. S. Inan (1997), A two-dimensional model of runaway electron beams driven by quasi-electrostatic thundercloud fields, *Geophys. Res. Lett.*, *24*, 2639–2642.

Lyons, W. A. (1994), Characteristics of luminous structures in the stratosphere above thunderstorms as imaged by low-light video, *Geophys. Res. Lett.*, *21*, 875–888.

Lyons, W. A. (1996), Sprite observations above the U.S. high plains in relation to their parent thunderstorm systems, *J. Geophys Res.*, *101*, 29,641–29,652.

Marshall, T. C., M. P. McCarthy, and W. D. Rust (1995), Electric-field magnitudes and lightning initiation in thunderstorms, *J. Geophys Res.*, *100*, 7097–7103.

Marshall, T. C., M. Stolzenburg, and W. D. Rust (1996), Electric field measurements above mesoscale convective systems, *J. Geophys Res.*, *101*, 6979–6996.

Pasko, V. P., and U. S. Inan (1994), Recovery signatures of lightning-associated VLF perturbations as a measure of the lower ionosphere, *J. Geophys. Res.*, *99*, 17,523–17,538.

Pasko, V. P., U. S. Inan, T. F. Bell, and Y. N. Taranenko (1997a), Sprites produced by quasi-electrostratic heating and ionization in the lower ionosphere, *J. Geophys Res.*, *102*, 4529–4562.

Pasko, V. P., U. S. Inan, and T. F. Bell (1997b), Sprites as evidence of vertical gravity wave structures above mesoscale thunderstorms, *Geophys Res. Lett.*, *24*, 1735–1738.

Pinto, O., Jr., et al. (2004), Thunderstorm and lightning characteristics associated with sprites in Brazil, *Geophys. Res. Lett.*, *31*, L13103, doi:10.1029/2004GL020264.

Raizer, Y. P. (1991), *Gas Discharge Physics*, Springer, New York.

Rakov, V. A., and M. A. Uman (2003), *Lightning: Physics and Affects*, Cambridge Univ. Press, New York.

Roussel-Dupre, R., and A. V. Gurevich (1996), On runaway breakdown and upward propagating discharges, *J. Geophys Res.*, *101*, 2297–2311.

Rowland, H. L. (1998), Theories and simulations of elves, sprites and blue jets, *J. Atmos. Sol. Terr. Phys.*, *60*, 831–844.

Sato, M., H. Fukunishi, M. Kikuchi, H. Yamagishi, and W. A. Lyons (2003), Validation of sprite-inducing cloud-to-ground lightning based on ELF observations at Syowa station in Antarctica, *J. Atmos. Sol. Terr. Phys.*, *65*, 607–614.

Sentman, D. D., E. M. Wescott, D. L. Osborne, D. L. Hampton, and M. J. Heavner (1995), Preliminary results from the Sprites94 aircraft campaign: 1. Red sprites, *Geophys. Res. Lett.*, *22*, 1205–1208.

Thomas, J. N., R. H. Holzworth, and J. Chin (2004), A new high-voltage electric field instrument for studying sprites, *IEEE Trans. Geosci. Remote Sens.*, *42*, 1399–1404.

Volland, H. (1984), *Atmospheric Electrodynamics*, Springer, New York.

Wescott, E. M., H. C. Stenbaek-Nielsen, D. D. Sentman, M. J. Heavner, D. R. Moudry, and F. T. São Sabbas (2001), Triangulation of sprites, associated halos and their possible relation to causative lightning and micrometeors, *J. Geophys Res.*, *106*, 10,467–10,477.

Williams, E. R. (1998), The positive charge reservoir for sprite-producing lightning, *J. Atmos. Sol. Terr. Phys.*, *60*, 689–692.

R. H. Holzworth, M. P. McCarthy, and J. N. Thomas, Department of Earth and Space Sciences, University of Washington, Condon Hall Room 310, Box 35130, Seattle, WA 98195–1310, USA. (bobholz@ess.washington.edu; mccarthy@ess.washington.edu; jnt@u.washington.edu)

O. Pinto Jr., National Institute of Space Research (INPE), Av. dos. Astronautas, 178, Caixa Posta 515, São Jose dos Campos, São Paulo 12201, Brazil. (osmar@dge.inpe.br)